Atherosclerosis 287 (2019) 122–133

Contents lists available at ScienceDirect

Atherosclerosis

journal homepage: www.elsevier.com/locate/atherosclerosis

Stimulation of alpha 7 nicotinic acetylcholine receptor (α7nAChR) inhibits atherosclerosis via immunomodulatory effects on myeloid cells

Marcus A. Ulleryd[a], Filip Mjörnstedt[a], Dimitra Panagaki[a], Li Jin Yang[a], Kajsa Engevall[a], Saray Gutiérrez[a], Yixin Wang[b], Li-Ming Gan[c,d], Holger Nilsson[a], Erik Michaëlsson[d], Maria E. Johansson[a,*]

[a] Department of Physiology, Institute of Neuroscience and Physiology, The Sahlgrenska Academy, University of Gothenburg, Gothenburg, Sweden
[b] Crown Bioscience Inc., Shanghai, China
[c] Department of Molecular and Clinical Medicine, Institute of Medicine, The Sahlgrenska Academy, University of Gothenburg, Gothenburg, Sweden
[d] Early Cardiovascular, Renal and Metabolism, R&D BioPharmaceuticals, AstraZeneca, Gothenburg, Sweden

HIGHLIGHTS

- The novel selective α7nAChR agonist AZ6983 decreases atherosclerosis in mice via immunomodulating effects.
- α7nAChR agonist AZ6983 enhances phagocytosis of apoptotic macrophages *in vitro*.
- α7nAChR agonist AZ6983 provides local anti-inflammatory effects in atherosclerotic lesions and in acute inflammatory models.
- α7nAChR agonist AZ6983 decreases inflammatory cytokines in human blood *in vitro*, and systemically *in vivo*.
- α7nAChR agonist AZ6983 can be an attractive therapeutic target for preventing atherosclerosis.

ARTICLE INFO

Keywords:
Alpha 7 nicotinic acetylcholine receptor
α7nAChR
Chrna7
Cholinergic signaling
Atherosclerosis
Immune responses
Phagocytosis
Inflammation
α7nAChR agonists
Cardiovascular disease

ABSTRACT

Background and aims: Alpha 7 nicotinic acetylcholine receptor (α7nAChR) stimulation can regulate acute inflammation, and lack of α7nAChR accelerates atherosclerosis in mice. In this study, we aimed to investigate the effects of the novel α7nAChR agonist, AZ6983, on atherosclerosis and assess its possible immunomodulating effects.

Methods: AZ6983 was tested *in vitro* in LPS-challenged mouse and human blood and *in vivo* using the acute inflammatory air pouch model. Thereafter, long-term effects of AZ6983 treatment on atherosclerosis and immune responses were assessed in *apoE*$^{-/-}$ mice after 8 and 12 weeks. Atherosclerosis was investigated in the aortic root and thoracic aorta, serum levels of cytokines were analysed and RNAseq was used to study aortic gene expression. Further, bone-marrow-derived macrophages were used to assess phagocytosis *in vitro*.

Results: α7nAChR activation by AZ6983 decreased pro-inflammatory cytokines in acute stimulations of human and mouse blood *in vitro*, as well as *in vivo* using the air pouch model. Treating *apoE*$^{-/-}$ mice with AZ6983 decreased atherosclerosis by 37–49% and decreased serum cytokine levels. RNAseq analysis of aortae suggested the involvement of several specific myeloid cell functions, including phagocytosis. In line with this, AZ6983 significantly increased phagocytosis in bone marrow-derived macrophages.

Conclusions: This study demonstrates that activation of α7nAChR with AZ6983 inhibits atherosclerosis in *apoE*$^{-/-}$mice and that immunomodulating effects on myeloid cells, such as enhanced phagocytosis and suppression of inflammatory cytokines, could be part of the athero-protective mechanisms. The observed anti-inflammatory effect in human blood supports the idea that AZ6983 may decrease disease also in humans.

* Corresponding author. Department of Physiology, Inst of Neuroscience and Physiology The Sahlgrenska Academy, University of Gothenburg, Box 432 405, 30, Göteborg, Sweden.
E-mail address: maria.e.johansson@neuro.gu.se (M.E. Johansson).

https://doi.org/10.1016/j.atherosclerosis.2019.06.903
Received 12 February 2019; Received in revised form 16 May 2019; Accepted 13 June 2019
Available online 15 June 2019

1. Introduction

Cardiovascular disease is the leading cause of death globally and atherosclerosis is often the underlying cause. Atherosclerosis is a chronic inflammatory disease, where both the innate and adaptive immune systems contribute to disease progression [1]. Autonomic dysfunction, usually manifested as increased sympathetic activity, has been associated with increased risk for both cardiovascular disease and atherosclerosis [2–4]. Recently, we demonstrated that autonomic dysfunction is associated with atherosclerosis and that inflammation could play an important role in mediating this relationship [5]. Interestingly, also the parasympathetic part of the autonomic nervous system has been implicated in regulating inflammation, i.e. the cholinergic anti-inflammatory pathway, where vagus nerve stimulation decreases inflammation in acute inflammatory disease via the activation of the alpha 7 nicotinic acetylcholine receptor (α7nAChR) [6,7]. Further, we have previously shown that α7nAChR can also modulate inflammation in more chronic diseases such as atherosclerosis, where lack of α7nAChR in hematopoietic cells dramatically accelerates atherosclerosis in mice [8]. However, the role of α7nAChR in atherosclerosis appears to be enigmatic. While we showed an anti-atherosclerotic effect of α7nAChR using a bone marrow transplantation model, this was not corroborated in a later study [9]. Additionally, even though Kooijman et al. did not detect a significant effect on atherosclerosis, using the bone marrow transfer strategy, they did show profound effects on immune reactivity, further supporting the role of α7nAChR in regulating inflammation [10]. Two recent atherosclerosis studies used the selective α7nAChR agonist ARR-17779 or the partial α7nAChR agonist GTS-21, demonstrating anti-atherosclerotic effects of α7nAChR stimulation in mice [11,12]. Yet, the specific mechanisms behind this athero-protective effect and the potency of other agonists remain to be investigated.

Atherosclerosis is characterized by the retention and accumulation of lipids within the vascular wall and the subsequent recruitment of immune cells to the site of inflammation. To orchestrate the recruitment of immune cells to the site of inflammation, chemotactic cytokines, i.e. chemokines, play a central role. Several chemokines have previously been implicated in the atherogenic process, including MCP1 (CCL2), RANTES (CCL5), MIP3a, CXCL1 (KC/Groα) and Fractalkine (CX3CL1) [13–17]. These chemokines and their receptors direct the recruitment of monocytes to the site of vascular inflammation. Once recruited to the vascular wall, monocytes can mature into macrophages and start engulfing modified lipoproteins, subsequently leading to foam cell formation [18]. Even though foam cell formation is a hallmark of plaque progression, macrophages have a complex role as they are professional phagocytes, important for scavenging modified lipoproteins, senescent cells and apoptotic cells [19].

We hypothesise that the athero-protective effect of α7nAChR stimulation is due to immunomodulatory mechanisms. The aim of the current study is to investigate if the novel agonist AZ6983 has an immunoregulatory role in human peripheral mononuclear cells *in vitro,* to test the agonist in an acute inflammatory model *in vivo,* and to investigate its pharmacological effect on atherosclerosis in *apoE*$^{-/-}$ mice.

2. Materials and methods

2.1. Experimental design

A novel selective agonist and modulator for the alpha 7 nicotinic acetylcholine receptor (α7nAChR), AZ6983 (Astra Zeneca, Gothenburg, Sweden), was studied *in vitro* using mouse and human whole blood. After confirming the anti-inflammatory effect of AZ6983 *in vitro,* we tested the compound in an acute inflammatory model, the air pouch model. Thereafter, we investigated its effect on atherosclerosis in *apoE*$^{-/-}$ mice, in two independent studies, for 12 and 8 weeks, respectively. The direct effect of AZ6983 on macrophage phagocytosis was investigated in bone marrow derived macrophages (BMDMs).

All animals were housed at 21–24 °C in a room with 12 h light/12 h dark cycle. Water and food were available *ad libitum*. All procedures involving mice were approved by the Regional Animal Ethics Committee at the University of Gothenburg, in accordance with the European Communities Council Directives of 22 September 2010 (2010/63/EU).

2.2. Compound AZ6983

The intrinsic activity of AZ6983 on α7nACh and α4β2nACh was tested in *Xenopus laevis* oocytes using two-electrode voltage-clamp recordings, and the affinity against α7nAChr, α3β4nAChR and 5-HT3aR was determined with competitive radioligand binding assays. For details, see Supplementary Data.

2.3. Ex vivo blood stimulations

Blood, from healthy donors of mixed age and gender, collected from the blood bank of Sahlgrenska hospital (n = 12), and from male *apoE*$^{-/-}$ mice through cardiac puncture (n = 11), was collected in heparin tubes. Human blood was divided into Eppendorf tubes in volumes of 500 µl and mouse blood in flat bottom well plates in volumes of 70 µl. Samples were challenged with 10 ng mL-1 of lipopolysaccharide (LPS, List Biological Laboratories Inc.) and treated with PBS or increasing concentrations of AZ6983, 0.1, 1, 10 or 100 µmol L-1. Control samples also included the addition of 100 µmol L-1 of AZ6983 to unstimulated blood. Samples were incubated for 4 h at 37 °C on a shaker and plasma was collected by centrifugation (20 min, 2600 g, RT). All samples were stimulated in duplicates and frozen at −20 °C until analysis. Cytokines were analyzed by commercially available ELISA kits using ELISA Ready-SET-go (eBioscience, Inc. San Diego, CA, US) for human TNF-α, IL-1β and IL-6, and ELISA MAXtm (BioLegend, San Diego, CA, US) for mouse TNF-α, according to the manufacturers protocol. Healthy donors have expressed both written and verbal consent for samples to be used in pharmacological research.

2.4. Air pouch model

To investigate whether AZ6983 affects acute inflammatory responses *in vivo,* we used the air pouch model in two separate experiments. At 8 weeks of age, male C57BL/6JRj mice (Janvier Labs, Le Genest-Saint-Isle, France) were injected with 3 ml of sterile air between the scapulae under isoflurane anesthesia. Three days later, the air pouch was re-filled with 3 ml of sterile air. On day six, mice received an i.p. injection of PBS (control), AZ6983 13.9 µmol kg-1 or AZ6983 139 µmol kg-1. After 15 min, all mice received LPS (10 µg, List Biological Laboratories Inc., Campbell, USA) into the pouch cavity. Mice were sacrificed 6 h or 24 h post LPS injection by an overdose of pentobarbital (i.p., Apoteket AB, Stockholm, Sweden). The 6 h time point was separated into two sacrifice days and the statistics adjusted accordingly. The pouch cavity was flushed with 2 ml of PBS with 1.6 mmol L-1 EDTA and the exudate collected. White blood cell count in the exudate was analyzed using the TC20 Automated Cell Counter (Bio-Rad, CA, US) and thereafter centrifuged for 5 min at 400*g*. Supernatants were stored for Multiplex analysis and cell pellets used for flow cytometry analysis.

2.5. Atherosclerosis studies

In an initial study, we investigated the effect of 12-week treatment with AZ6983 on atherosclerosis (referred to as the 12-week study). *apoE*$^{-/-}$ mice on C57BL/6 background were bred and kept at the Beijing Medical University animal center. The study was performed at the CrownBio International R&D Center, Beijing, China. At 7 weeks of age, male mice were randomly divided into 2 groups: A/Control diet

(n = 12) and B/AZ6983 admixed in diet to yield a daily dose of 50 μmol kg-1 (n = 12). From 8 weeks of age, all mice were fed a high fat, cholesterol enriched diet (21% fat, 0.15% cholesterol; R638, Lantmännen, Sweden) with or without the α7nAChR agonist AZ6983 for 12 weeks.

To characterize the mechanisms behind the atheroprotective effects of AZ6983 at an earlier time point, we next performed an 8 week study (Referred to as the 8-week study). Male *apoE*$^{-/-}$ mice from Taconic (C57BL/6 background, B6192P2-Apoe^{tm1Unc}N11, Taconic, Denmark) were kept at the Laboratory for Experimental Biomedicine, Gothenburg, Sweden. At 7 weeks of age, mice were randomly divided into two groups: i/Control (n = 14) and ii/α7nAChR agonist AZ6983 (n = 15). At 10 weeks of age, mice were anesthetized using isoflurane for 5–10 min and subcutaneously implanted with osmotic minipumps (Alzet model 2004, DURECT Corporation, ALZET Osmotic Pumps, Cupertino, CA, USA) delivering vehicle (28% cyclodextrin in saline), or α7nAChR agonist AZ6983 (50 μmol kg-1 per day) for 8 weeks. Due to the duration of the minipumps, replacement was done after 4 weeks. From 10 weeks of age and throughout the experiment, mice were fed a high fat, cholesterol enriched diet (21% fat, 0.15% cholesterol; R638, Lantmännen, Sweden). Both groups included mice with reactions to the minipumps and had to be re-sutured to ensure proper treatment. If not possible, mice were excluded from the study (included/excluded, n = 20/9).

2.6. Tissue preparation

The vascular tree was perfused by intracardiac saline infusion to clear the lumen from blood at 100 mmHg. For the 12-week study, the heart and aorta were dissected, fixated in 4% neutral phosphate buffered formaldehyde for one week, and used for *en face* quantification. For the 8-week study, one third of the spleen was kept in PBS on ice for subsequent flow cytometry analysis. The heart and aortic root were embedded in Optimal Cutting Temperature Compound (OCT), and cryosectioned for immunohistochemistry while the aorta and remaining spleen were snap-frozen and stored at −80 °C for RNA isolation.

2.7. Atherosclerotic lesion analysis

Aortas from the 12-week study were prepared as previously described [20], and mounted with glycine gelatin with the lumen side facing upward. Images of the whole-mounted aorta were captured using a camera. The total area of the aorta was manually outlined by a blinded observer and lesions automatically computed by morphometry (BioPix, Gothenburg, Sweden). The aortic root from the 8-week study was serially sectioned at six different levels, 200–700 μm from the aortic valves. Sections were air-dried, fixed with 4% formaldehyde in PBS and then stained with ORO for lipids. Images were captured with an Olympus BX60F5 microscope, connected to an Olympus DP72 camera. Lesions were manually outlined and measured by a blinded observer. Lesion area and lipid accumulation were computed by an image analysis program (CellSens Dimension Desktop 1.5, Version 1.5, Olympus Optical Company, Hamburg, Germany), and the area was normalized to the external elastic lamina (EEL).

Immunostaining was performed on acetone-fixed cross-sections of the aortic root as previously described [8]. The following antibodies were used: anti-CD68 (MorphoSys UK Ltd, Oxford, UK), anti-Ki67 (ABCAM, Cambridge, UK), anti-CD47 (R&D Systems, Minneapolis, US), anti-VCAM-1 (Hycult Biotech, Uden, Netherlands), anti-CD3 (Abcam), anti-I-Ab (BD Biosciences, Franklin Lakes, NJ, US), anti-MCP1 (Abcam) and anti-CXCL1 (Abcam). Sections were incubated with a biotinylated secondary antibody (Vector Laboratories) followed by incubation with Vectastain ABC reagent (Vector Laboratories). Binding was visualized using the NOVA RED kit (Vector Laboratories), counterstained with Hematoxylin (HARRIS HTX Histolab: Histolab Procuts AB, Gothenburg, Sweden) and mounted with Kaisers Glyceringelatine (Merck Millipore, Darmstadt, Germany). A Rat IgG isotype (R&D Systems) or Rabbit IgG (Abcam) served as negative control. Images were captured and staining was computed as described above. Staining was normalized to EEL and expressed as area or number of cells.

2.8. In vivo blood analysis

Total cholesterol, free cholesterol and low-density-lipoprotein (LDL) in plasma (12-week study) or serum (8-week study) was determined using a colorimetric end-point assay (ab65390 HDL and LDL/VLDL Cholesterol Assay Kit, Abcam, Cambridge, UK) according to the manufacturer's protocol. In brief, the enzyme mix specifically binds to free cholesterol and reacts with a probe to develop a color that can be detected at 570 nm. Total cholesterol or free cholesterol was detected separately by the addition or absence of cholesterol esterase that hydrolyzes cholesteryl esters into free cholesterol. LDL fraction was separated from HDL by using the precipitation buffer. Serum creatinine was determined colorimetrically at 485 nm by Jaffe's reaction. Briefly, equal amounts of NaOH (1 M) and picric acid (1%) was mixed into serum samples and creatinine standards (C3613-1 SET, Sigma-Aldrich, St. Louis, US) and the concentrations calculated after spectrophotometric detection. Alanine transaminase (ALT) was colorimetrically analyzed using the Mouse ALT ELISA kit EKM1658 (Nordic Biosite, Täby, Sweden) according to the manufacturers protocol. Briefly, biotin conjugated anti-ALT antibody was added to the serum samples and standards. Following incubation and washing, HRP-streptavidin was added and unbound conjugates were washed away. The addition of TMB, followed by a stop solution, produces a yellow color that was colorimetrically analyzed at 450 nm. AZ6983 drug exposure was determined in plasma and in whole blood for the 12-week study and the 8-week study, respectively, by liquid chromatography–mass spectrometry. Briefly, samples were haemolysed and precipitated with acetonitrile (Fisher Scientific, Waltham, MA, US). After centrifugation, the supernatant was diluted with 0.2% formic acid (Merck, Darmstadt, DE). Analysis was performed on a short reversed-phase HPLC-column, Xbridge C18, with rapid gradient elution and MSMS detection using a triple quadrupole instrument with electrospray ionization, and Selected Reaction Monitoring (SRM) acquisition analyzed with MassLynx, version 4.1 (Waters Corporation, Milford, MA, US)

2.9. RNA isolation, cDNA synthesis, and real-time PCR analysis

RNA of thoracic aorta, spleen and aortic lymph nodes was extracted by using the RNAeasy® Fibrous Tissue Mini Kit and miRNeasy® Mini Kit (Qiagen GmbH, Hilden, Germany) according to the manufacturer's protocol. Concentration and quality were analyzed using a NanoDrop (NanoDrop Products, DE, US) and electrophoresis (Experion, Bio-Rad Laboratories, CA, USA). Reverse transcription was performed using the QuantiTect Reverse Transcription Kit (Qiagen GmbH, Hilden, Germany) according to the manufacturer's protocol. Gene expression of inflammatory markers in spleen was determined with real-time PCR (LightCycler, Roche Diagnostics GmbH, Mannheim, Germany) utilizing SYBR-Green I (QuantiFast SYBR® Green PCR Kit, Qiagen). Using the GenEx Standard software (TATAA Biocenter, Gothenburg, Sweden) *Ywhaz* was suggested as references gene and subsequently used in the analysis of mRNA levels in spleen. Gene expression levels were analyzed using the GenEx Standard software as previously described [8]. Samples with replicates diverging more than 1.0 Ct were excluded.

2.10. Flow cytometry analysis

Spleens were homogenized in CellWASH (BD Biosciences, Franklin Lakes, NJ, USA), using cell strainers. After centrifugation, splenocyte and exudate pellets were resuspended in lysis buffer (BD Biosciences) for 6 min on ice. Hemolysis was stopped by adding CellWASH (BD Biosciences), followed by centrifugation and resuspension. 3×10^5 cells/

sample were used for staining. Following incubation with Fc-block (2.4G2; BD Biosciences), splenocytes were incubated with the following antibodies: anti-CD3-PerCp-Cy5.5 (clone 145-2C11), anti-CD11b-Alexa Flour 488 (M1/70) and Ly6G-PE (AL-21). For flow cytometry analysis of the air pouch exudate, the following antibodies were used: anti-CD3-PE (145-2C11), anti-CD11b-APC (M1/70) and anti-Ly6G-FITC (1A8), all from BD Biosciences. Cells were acquired using FACSCantoA or FACSCantoII flow cytometers (BD Biosciences) and data analyses performed with FACSDiva software (version 6.1.3; BD Biosciences) for splenocytes and BMDMs with beads, or FlowJo software (version 10.4.2; FlowJo, LLC) for air pouch exudate and BMDMs with apoptotic cells.

In the analysis, a leukocyte gate included the cells of interest. T cells were defined as $CD3^+$ cells, monocytes as $CD11b^+$ cells with low granularity or as $CD11b^+$ + $Ly6G^-$ cells. Monocytes were subsequently defined as $Ly6C^{high}$ or $Ly6C^{low}$. Neutrophils were defined as $Ly6G^+$ cells. Flow cytometry results are presented as frequencies of parent population, immune cell count by multiplying the frequencies to white blood cell count or mean fluorescence intensity (MFI) to assess the individual phagocytic capacity of each macrophage. For representative gating strategy, see Supplemental Fig. II-IV.

2.11. Multiplex analysis of the air pouch exudate and serum

The Bio-Plex ProTM Mouse Chemokine Panel 33-plex (#12002231, Bio Rad Laboratories, Inc. Hercules, USA) was used to quantify chemokines and cytokines in the air pouch exudate and serum samples from the 8-week study. The assay was performed according to the manufacturers' protocol. 33 chemokines and cytokines were quantified, including; Eotaxin, Fractalkine, GM-CSF, CCL1, IFNg, IL-6, CXCL10, MIP3a, CCL17 and TNFα.

2.12. Differentiation of primary bone marrow derived macrophages and phagocytosis assay

Primary bone marrow derived macrophages (BMDMs) were isolated from 8 to 18 week old male and female *apoE*$^{-/-}$ (Taconic, Denmark) and *LDLr*−/− mice (in-house breeding). Mice were sacrificed by an i.p. injection of pentobarbital (Apoteket AB). The bones of the hind legs were dissected, washed with EtOH (70%) and rinsed in sterile PBS. Femur and tibia was separated and bone ends were cut before flushing out the bone marrow using a syringe filled with RPMI. Cells were cultured in petri dishes with differentiation medium (RPMI containing 10% FBS, 1% penicillin/streptomycin and M-CSF Recombinant Murine M-CSF, PeproTech Nordic, Stockholm, Sweden), at 37 °C and 5% CO2. At day 2 unattached cells were collected and re-seeded into the petri dishes together with fresh differentiation medium. At day 6 medium was discarded and cells harvested in ice cold PBS using cell scrapers. After centrifugation cells were resuspended in differentiation medium and plated for phagocytosis assay.

Primary BMDMs were seeded into 12-well plates (250 000 -500 000 cells/well) with differentiation medium, treated with or without AZ6983 in 3–5 replicates at a concentration of 0.5 or 5 μmol L-1, and incubated at 37 °C and 5% CO_2 for 24 h. Unattached cells were discarded and phagocytosis of beads was tested by adding 10 FITC-labeled latex beads/cell (Polysciences Europe, Hirschberg, Germany) in complete RPMI (RPMI with 10% FBS, 1% penicillin/streptomycin) for 45 min at 37 °C. Plates were placed on ice to stop phagocytosis and cells were washed with RPMI to discard non-phagocytosed beads before they were resuspended in CellWASH by gentle scraping. Phagocytosis of apoptotic macrophages was assessed by incubating a set of BMDMs with 10 μM Dexamethasone (cat: 1126/100, Tocris, Abingdon, UK), to induce cell death, in differentiation medium for 6 h at 37 °C, with the subsequent addition and incubation of Far Red Viability dye (L34973, ThermoFischer Scientific) for 30 min at 4 °C. Healthy BMDMs were labeled with 10 μmol L-1 of CellTracker Green-Bodipy (cat: C2102, ThermoFischer Scientific) for 30 min at 37 °C and 5% CO_2. Far Red labeled apoptotic cells were added to the Green-Bodipy-labeled healthy macrophages for 2 h at 37 °C and 5% CO_2 before all cells were gently scraped and collected. The ratio of phagocyting macrophages and their phagocyting capacity was measured in a flow cytometer, as described above. Experiments were repeated at 5-7 independent time points and an average of replicates was calculated for each experiment. Flow cytometry results are presented as percentages of macrophages that are positive for fluorescent latex beads or apoptotic cells and mean fluorescence intensity (MFI) of cells positive for FITC-labeled latex beads or Far Red Viability-labeled apoptotic macrophages.

2.13. Statistics

Data were tested for normality and statistical methods chosen according to the outcome. Lesion area in aortic root was analyzed with repeated measurement 2-way Anova. Mean lesion area in aortic root and thoracic aorta was analyzed with Students t-test. Data on immunohistochemistry, flow cytometry of splenocytes, cholesterol, ALT, creatinine, spleen weight and body weight was analyzed with Mann-Whitney *U* test. Gene transcription in spleen was analyzed with Mann-Whitney *U* test, followed by Holm's sequential Bonferroni correction. Flow cytometry data from phagocytosis experiments and cytokine response in blood (logarithmically transformed for normality) were analyzed with repeated measurement 1-way Anova followed by Holm -Sidak's multiple comparison test. Flow cytometry data, cell count and cytokine multiplex from both air pouch experiments were logarithmically transformed for normality. The 6 h time point was analyzed and expressed as estimated marginal means ± 95% confidence interval (95% CI) to adjust for sacrifice. The 24 h time point was analyzed with the 1-way Anova followed by Holm -Sidak's multiple comparison test and expressed as mean ± a 95% CI. Serum cytokine multiplex data was analyzed with Mann-Whitney *U* test. Differences in sample numbers were due to laboratory errors or lack of sample material. Statistical outliers, detected by the software, were excluded from the analysis. Unless otherwise stated, data is expressed as mean ± SEM. All tests were two sided and $p < 0.05$ was considered significant for all data. The statistical analyses were carried out with the GraphPad Prism software (Version 5.03, La Jolla, CA, USA) or IBM SPSS (IBM SPSS Statistics for Windows, Version 25.0. Armonk, NY: IBM Corp).

3. Results

3.1. Compound: AZ6983

The novel selective α7nAChR agonist AZ6983 (Supplemental Fig. 1A), (((R)-5-(2-(pyridin-3-yl)oxazol-5-yl)-3H-1′-azaspiro[furo[2,3-b]pyridine-2,3′-bicyclo[2.2.2]octane] [21] (Astra Zeneca, Gothenburg, Sweden) was used throughout this study. AZ683 is an orthosteric agonist for α7nAChR that acts in synergy with acetylcholine (ACh) (Supplemental Figs. 1A–C). The compound did not evoke any activation of the acetylcholine receptor α4β2nAChR (data not shown). AZ6983 affinity for the target receptor α7nAChR was measured using a competitive radioligand binding assay and compared to two associated receptors, the acetylcholine receptor α3β4nAChR, and the biochemically homologous 5HT3aR. IC_{50} for α7nAChR was 19 nmol L-1 with a high selectivity over α3β4nAChR (4.9 μmol L-1), and the serotonin receptor 5HT3aR (6.6 μmol L-1) (Supplemental Table I). The purity of the compound used in this study was determined to be 99.6% using high-performance liquid chromatography.

3.2. α7nAChR agonist AZ6983 decreases pro-inflammatory cytokines in whole blood samples

To first test the immunoregulatory effects of the α7nAChR agonist AZ6983, cytokine secretion was analyzed in LPS-challenged mouse and human whole blood. AZ6983 decreased TNFα levels in a dose-

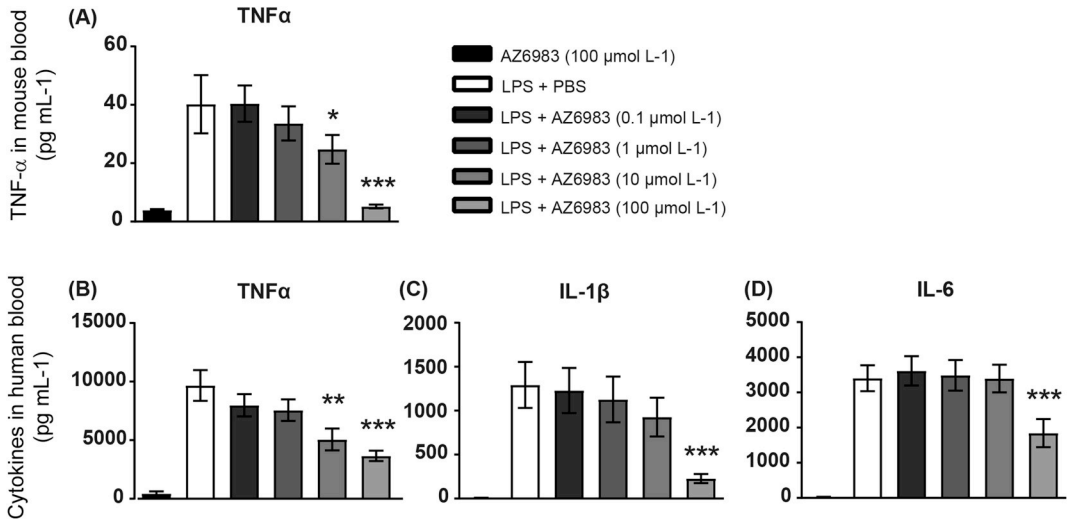

Fig. 1. AZ6983 inhibits inflammatory cytokine production in blood from humans and mice *ex vivo*.
(A-D) Blood from *apoE*$^{-/-}$ mice and healthy human donors was stimulated with 10 ng mL-1 of lipopolysaccharide (LPS) together with PBS, or increasing concentrations of α7nAChR agonist AZ6983 (0.1, 1, 10 and 100 μmol L-1). Control samples (black bars) were stimulated with 100 μmol L-1 of AZ6983. Samples were incubated for 4 h and inflammatory cytokines assessed in plasma using ELISA. (A) TNF-α in mouse blood (n = 11). (B-D) TNF-α, IL-1β and IL-6 in human blood (n = 12). Bars represent cytokine concentrations in pg mL-1 and are expressed as mean ± SEM. *$p < 0.05$, **$p < 0.01$, ***$p < 0.001$.

dependent manner in both mouse (Fig. 1A) and human (Fig. 1B) whole blood at both 10 and 100 μmol L-1. IL-1β and IL-6 were only significantly decreased at 100 μmol L-1 (Fig. 1C and D).

3.3. α7nAChR agonist AZ6983 decreases inflammatory cytokines in vivo in the air pouch model

We next sought to test the effects of the α7nAChR agonist AZ6983 in an *in vivo* model of acute inflammation by using the air pouch model. After 6 h of inflammation, AZ6983 significantly decreased the concentration of several cytokines at both 13.9 μmol kg-1 and 139 μmol kg-1 in the air pouch exudate compared to the untreated mice (Fig. 2A). Following the *post hoc* analysis, the concentration of following chemokines and cytokines was found significantly decreased compared to untreated mice; CXCL10, TNFα, MIP3a and CCL1 (Fig. 2B). There was no significant difference in white blood cell count in the air pouch exudate after using any of the different doses of AZ6983 (Fig. 2C, upper panel), neither in the cell count of CD3$^+$ T cells, Ly6G$^+$ neutrophils nor in CD11b$^+$ monocytes (Fig. 2D, upper panel). To assess the immune cell composition at a later time point, a separate air pouch experiment was conducted where mice were sacrificed at 24 h after inflammation. Similar to the 6 h time point, no changes in white blood cell count, CD3$^+$ T cells, Ly6G$^+$ neutrophils or CD11b$^+$ monocytes were found (Fig. 2C and D, lower panel). However, AZ6983 at the 13.9 μmol kg-1 dose caused a 48% decrease in the number of CD11b$^+$ monocytes, yet, this did not reach statistical significance.

3.4. α7nAChR agonist AZ6983 decreases atherosclerosis in apoE$^{-/-}$ mice

After confirming the anti-inflammatory effects of AZ6983 *in vitro* and in an acute *in vivo* model, we next investigated whether the immunomodulating effects could affect atherosclerosis progression in mice. In the first study, treatment with AZ6983 admixed in food for 12 weeks reduced the atherosclerotic lesion area by 49% in the thoracic aorta compared to controls (Fig. 3A). To verify this finding, we performed an 8-week study with administration of AZ6983 by osmotic minipumps. Here, atherosclerotic lesion area was decreased by 37% in the aortic root and lipid accumulation in lesions by 48% compared to controls (Fig. 3B–E). When investigating plaque morphology, AZ6983 treated mice had a 47% reduction in CD68$^+$ macrophages compared to untreated mice (Fig. 3F), however, the amount of CD3$^+$ T cells was not altered (Fig. 3G). Further characterization of plaque composition showed no difference in the expression of vascular adhesion molecule VCAM-1 (Fig. 3H), nor in the MHC class II marker I-Ab between the groups (Fig. 3I). Besides immune cell infiltration and activation, cellular proliferation is an important contributor to plaque progression. We therefore investigated the expression of the proliferation marker Ki67 in the aortic root. AZ6983 decreased Ki67 by 49% compared to untreated mice (Fig. 3J). Another contributing factor to plaque progression is failure in removing apoptotic cells from the vessel wall, i.e. efferocytosis [22]. We therefore analysed the expression of the anti-phagocytic marker CD47. Interestingly, AZ6983 decreased CD47 expression by 58% (Fig. 3K). In regard to the reduction of macrophage marker CD68, we also stained for two monocyte recruiting chemokines. AZ6983 treatment reduced the monocyte chemoattractant protein-1 (MCP1) by 44% and did not have any significant effect on CXCL1 in the lesions (Fig. 3L and M, respectively).

To further investigate potential cellular processes as mediators of AZ6983 treatment effects, we performed RNA sequencing of aortas from the 8 week study. Ingenuity Pathway Analysis of the differentially expressed genes (See table in Ref. [23]) suggested that the top 5 specific functions regulated by AZ6983 treatment were phagocytosis of cells, arteriosclerosis, engulfment of cells, adhesion of blood cells and binding of myeloid cells (Supplemental Table II). Since both phagocytosis and engulfment of cells were among the top regulated functions, and we previously observed decreased expression of the anti-phagocytic marker CD47, this prompted us to investigate the effects of AZ6983 on phagocytosis using bone marrow derived macrophages (BMDMs). AZ6983 increased the frequency of BMDMs with the capability to engulf latex particles and their fluorescence intensity, as an indication of the amount of beads each macrophage can engulf (Fig. 3N). Also, the frequency of BMDMs with capability to engulf apoptotic macrophages was increased (Fig. 3O, left panel). In regard to apoptotic macrophages, the phagocytic capacity of BMDMs was not affected by the treatment (Fig. 3O, right panel)

3.5. α7nAChR agonist AZ6983 decreases systemic inflammation in vivo

Systemic immune-regulating effects of AZ6983 administration in *apoE*$^{-/-}$ mice were assessed in the 8-week study. Multiplex analysis of serum samples showed that AZ6983 treatment had a suppressive effect on pro-inflammatory cytokines (Fig. 4A), specifically indicating MIP3α,

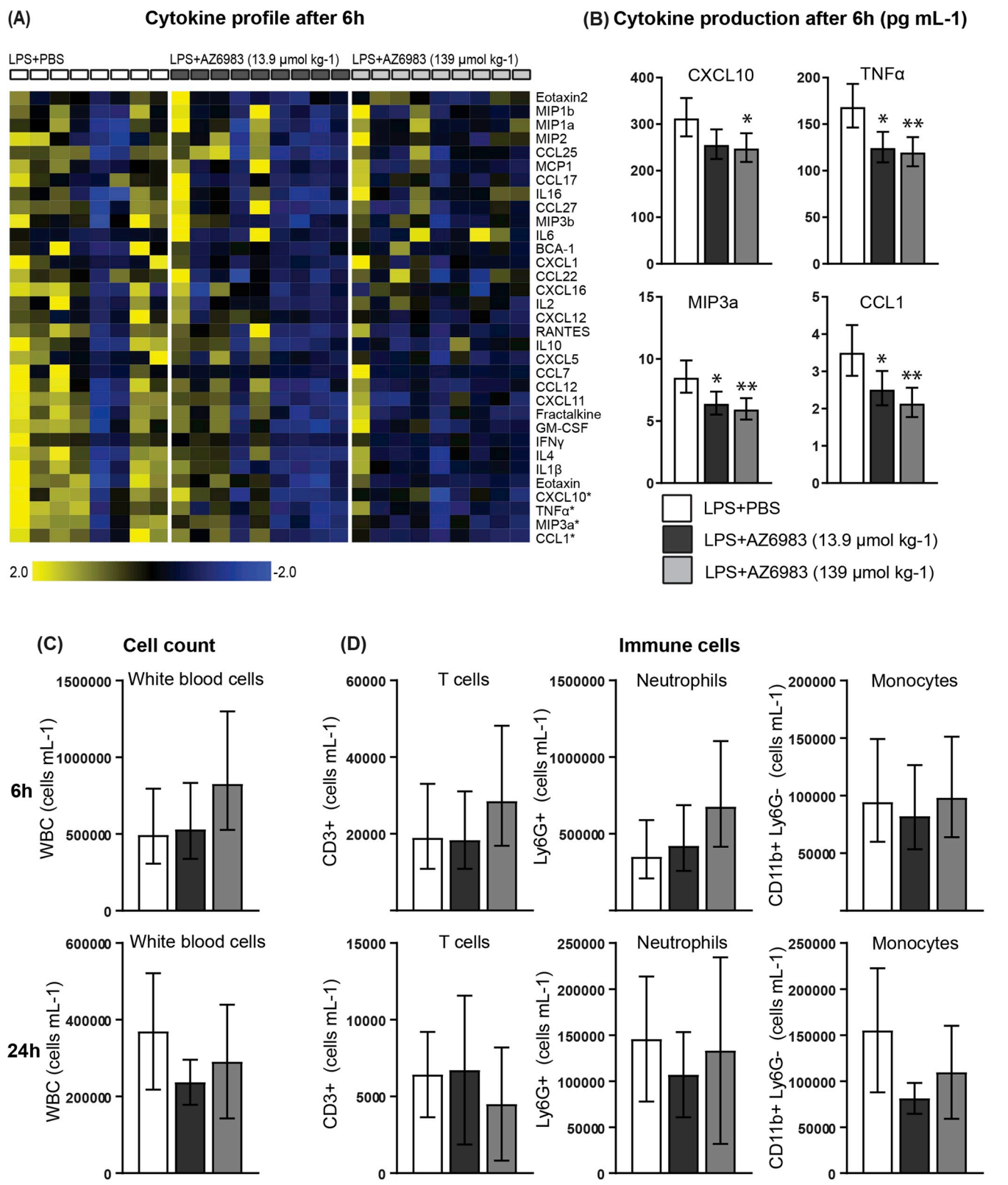

Fig. 2. AZ6983 decreases inflammation in air pouch model.
Acute immunomodulatory properties of AZ6983 were tested using the air pouch model in C57BL/6JRj mice. Mice were treated with PBS, AZ6983 (13.9 µmol kg-1), or AZ6983 (139 µmol kg-1) i. p. and subsequently challenged with LPS into the pouch for 6 h or 24 h. Cytokine concentration in the air pouch-exudate was analyzed after 6 h by Luminex and presented as a heatmap (A) with * indicating significant differences between the groups using estimated marginal mean to adjust for sacrifice day. (B) Graphs representing estimated marginal means of cytokines that were significantly different compared to the controls. (C) White blood cell count and (D) cell count of specific immune cells in the air pouch exudate after 6 h (upper panel), presented as estimated marginal mean, and after 24 h, (lower panel) presented as mean. Error bars represent a 95% CI.*$p < 0.05$, **$p < 0.01$, n = 8–9 per group.

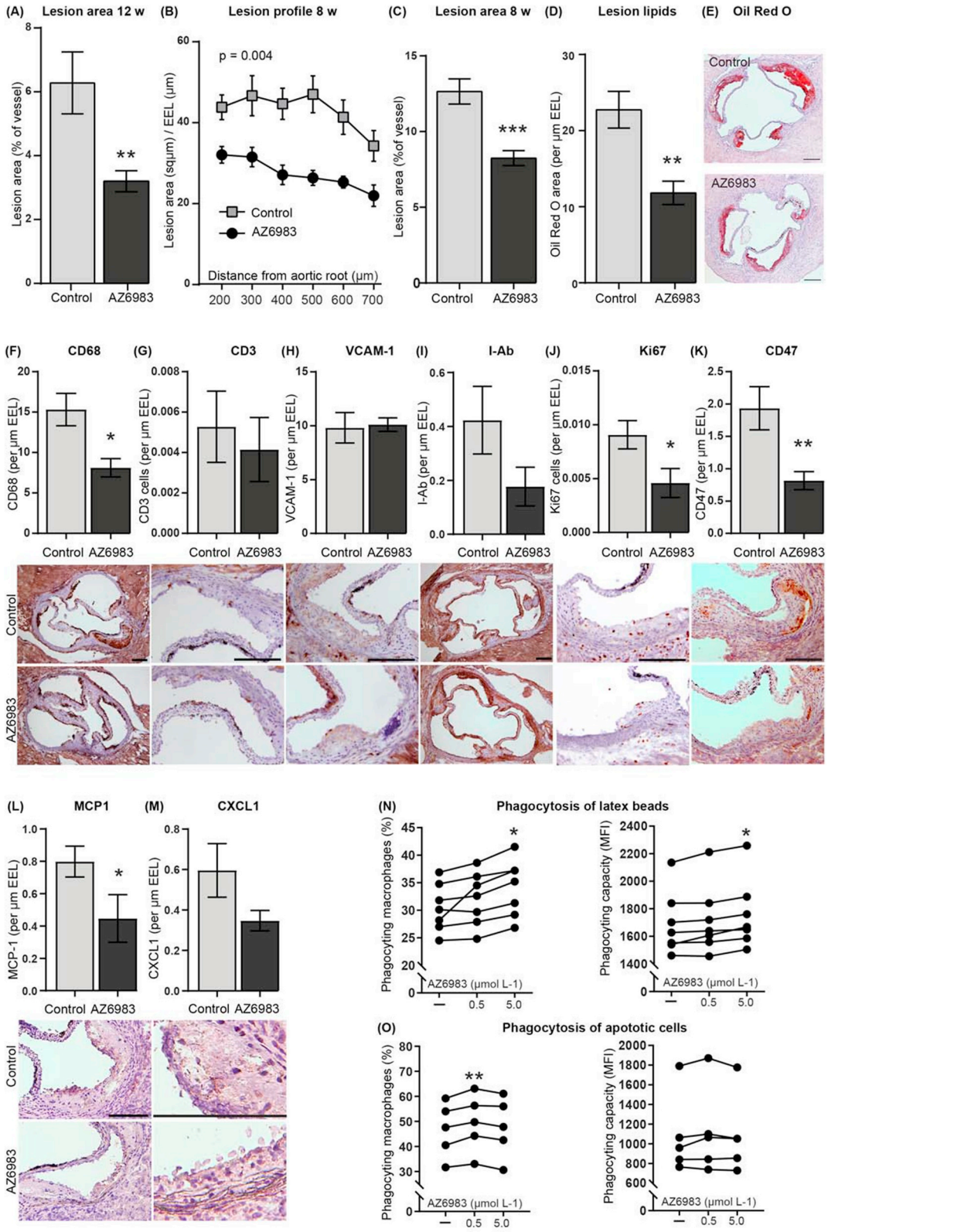

(caption on next page)

Fig. 3. The α7nAChR agonist AZ6983 reduces atherosclerosis in *apoE*$^{-/-}$ mice and improves phagocytosis *in vitro*.
(A) *apoE*$^{-/-}$ mice received α7nAChR agonist AZ6983, 50 μmol kg-1 per day, admixed in Western diet or regular Western diet for 12 weeks. *En face* quantification of thoracic aorta after oil red O staining. Graph represents the percentage of lesion area of total vessel area (n = 12 for both groups). (B-E) *apoE*$^{-/-}$ mice treated with 50 μmol kg-1 per day of AZ6983 or vehicle in osmotic minipumps for 8 weeks. Atherosclerosis was measured in serial sections of the aortic root. (B) Lesion area for all sections normalized to external elastic lamina (EEL) and (C) mean lesion area of all sections as % of total vessel area. (D) Lipid accumulation was detected with Oil Red O and is presented as stained area normalized to EEL. (E) Representative micrographs of Oil Red O stained sections. (F-K) Quantification of immune markers in lesions of the aortic root after 8 weeks of treatment with AZ6983. (F) Macrophage stained area (CD68), (G) T cells (CD3), (H) vascular cell adhesion protein-1 (VCAM-1), (I) MHC class II (I-Ab), (J) proliferating cells (Ki67), (K) anti-phagocytic protein (CD47), (L) monocyte chemoattractant protein-1 (MCP1) and (M) the chemokine CXCL1 stained area are normalized to EEL and presented in graphs together with representative micrographs below (n = 8–11/group). (N-O) Bone-marrow-derived macrophages were stimulated with PBS, 0.5 or 5.0 μmol L-1 of α7nAChR agonist AZ6983 in replicates for 24 h. The following day labeled latex beads were added for 45 min or labeled apoptotic macrophages were added for 2 h before assessing phagocytosis by flow cytometry. Graphs represent the frequency of phagocytic cells (left panels) and their capacity (right panels), assessed by the mean fluorescence intensity, to phagocyte beads or apoptotic macrophages. Each experiment included 3-5 replicates for all conditions and mean values are represented as dots. Experiments were repeated at 5-7 different days and are represented with connected lines where * indicates significant differences between the marked treatment group and control group using repeated measurement 1-way Anova followed by Holm -Sidak's multiple comparison test, *$p < 0.05$, **$p < 0.01$. Scale bar represents 200 μm . (For interpretation of the references to color in this figure legend, the reader is referred to the Web version of this article.)

IL-4, RANTES (CCL5), MCP1 (CCL2), CXCL1 (GROα), Eotaxin 2 (CCL24) and fractalkine (CX3CL1) as significantly reduced compared to untreated mice (Fig. 4B). Immune responses were also analyzed in spleens, an important source of cells responding to inflammation, and identified as a significant site for α7nAChR-modulated immune responses [24]. Real time PCR revealed reduced gene expression of CD86, CD4, CD8, and IFNγ after treatment with AZ6983 (Fig. 4C), markers associated with T cells and their activation. There were no differences in gene expression of CD3, TNFα, IL-1β, IL-6, MCP1, CCL5 and CCR2 between the treatment groups. (Fig. 4C). Mice treated with AZ6983 showed an increased spleen weight compared to controls (Fig. 4D). Splenocytes were further characterized by flow cytometry. AZ6983 treatment reduced the frequency of $CD3^+$ T cells whereas the frequency of $CD11b^+$ cells was increased compared to controls (Fig. 4E and F). Moreover, AZ6983 increased the frequency of $Ly6C^{high}$ monocytes, and decreased the frequency of $Ly6C^{low}$ monocytes in the spleen (Fig. 4G and H).

3.6. Cholesterol, body weight, AZ6983 exposure and biomarkers of specific organ disorders

Total cholesterol levels in plasma or serum were measured in both atherosclerosis studies. After 8 weeks, total cholesterol was increased in AZ6983 treated animals in the 12-week study, and decreased in the 8-week study (Table 1). At sacrifice, no differences were seen between the control group and the treatment group in the 12-week study (Table 1). Free cholesterol and LDL cholesterol were assessed in the 8-week study and were both decreased in the treatment group compared to controls (Table 1). Mean AZ6983 exposures in the treatment groups were 0.37 μmol L-1 in the 12-week study, and 0.56 μmol L-1 in the 8-week study (Table 1). Treatment with AZ6983 was not associated with any changes in body weight or biomarkers for liver damage and kidney function, alanine transaminase (ALT) and creatinine, respectively (Table 1).

4. Discussion

In the current study, activation of α7nAChR with AZ6983 decreased atherosclerosis in *apoE*$^{-/-}$ mice in two independent studies, both in the aortic root and thoracic aorta. Further, AZ6983 reduced pro-inflammatory cytokine levels and modulated myeloid immune responses in *apoE*$^{-/-}$ mice. Importantly, AZ6983 also reduced cytokine levels in human immune cells. This study adds knowledge on the mechanisms behind the athero-protective effect of α7nAChR stimulation. Hence, this study further supports that activation of α7nAChR is a potential target for athero-protective interventions and adds AZ6983 as a potent pharmacological candidate that acts via immunomodulatory effects.

By stimulating α7nAChR with AZ6983 *in vitro,* we demonstrate anti-inflammatory effects of the novel agonist on human peripheral immune cells. This supports previous studies in samples from healthy volunteers as well as patients with rheumatoid arthritis, where stimulation of α7nAChR using nicotine or GTS-21 reduced pro-inflammatory cytokines in whole blood assays [25,26]. In the present study, the anti-inflammatory effects of AZ6983 were further tested *in vivo* using the acute air pouch model. This model is used in atherosclerosis studies due to its resemblance to microvascular inflammation [27–30]. We show that AZ6983 suppressed several pro-inflammatory cytokines, including: CCL1, CXCL10, MIP3α (CCL20) and TNFα [14,31–34] after 6 h of inflammation. Taken together, the affected cytokines indicate a general reduction in myeloid cell response. Still, the number of $CD11b^+$ monocytes in the air pouch exudate was unaffected by the treatment. Since similar studies measured monocyte recruitment at 20–24 h after the inflammatory challenge [27–30], we followed up with a cell recruitment assessment 24 h after inflammatory challenge. Surprisingly, despite a numerical reduction by 48% in monocyte recruitment, the statistical difference was nonsignificant.

Our findings on the acute anti-inflammatory properties of AZ6983 encouraged us to move further by testing the long-term effects of AZ6983 on atherosclerosis and investigating the potential underlying immune mechanisms. In two separate studies, we demonstrate that activation of α7nAChR with the novel agonist AZ6983 reduced the development of atherosclerosis. These findings support recent studies where α7nAChR agonists ARR-17779 and GTS-21 were used to determine α7nAChR-mediated inhibition of atherosclerosis in mice [11,12]. However, GTS-21 is considered a partial agonist to α7nAChR that also shows inhibitory effects on α4β2nAChR [35,36] and was recently shown to have anti-inflammatory effects independently of α7nAChR [37]. ARR-17779, on the other hand, is a full agonist for α7nAChR, with high selectivity over α4β2nAChR [38]. ARR-17779 belongs to the spirocyclic oxazolidinones, a group of compounds that has experienced challenges with cross reactivity to the 5HT3 receptors [39], however, ARR-17779 does not seem to have any cross reactivity with 5HT3R [40]. In the present study, increasing concentrations of AZ6983 potentiated the response to ACh and elicited agonistic properties by itself in oocytes expressing α7nAChR. Further, AZ6983 showed a high selectivity over $5HT3_aR$ and α3β4nAChR, and did not evoke any response in α4β2nAChR-expressing oocytes. Despite inconclusive data on the effects of α7nAChR-ablation [8–10], the present study adds robustness to the univocal atheroprotective role of α7nAChR-stimulation [11,12] by contributing with a new selective agonist. The comparatively higher concentrations needed to suppress cytokines *in vitro*, compared to the *in vivo* experiments, may be explained by AZ6983 being an orthosteric modulator that only function as a partial agonist in the absence of endogenous ACh. However, in comparison with *in vitro* studies using GTS-21 [26], AZ6983 effectively depresses cytokine levels at lower concentrations.

Even though two previous studies demonstrated an anti-atherosclerotic effect of α7nAChR stimulation, the underlying mechanism

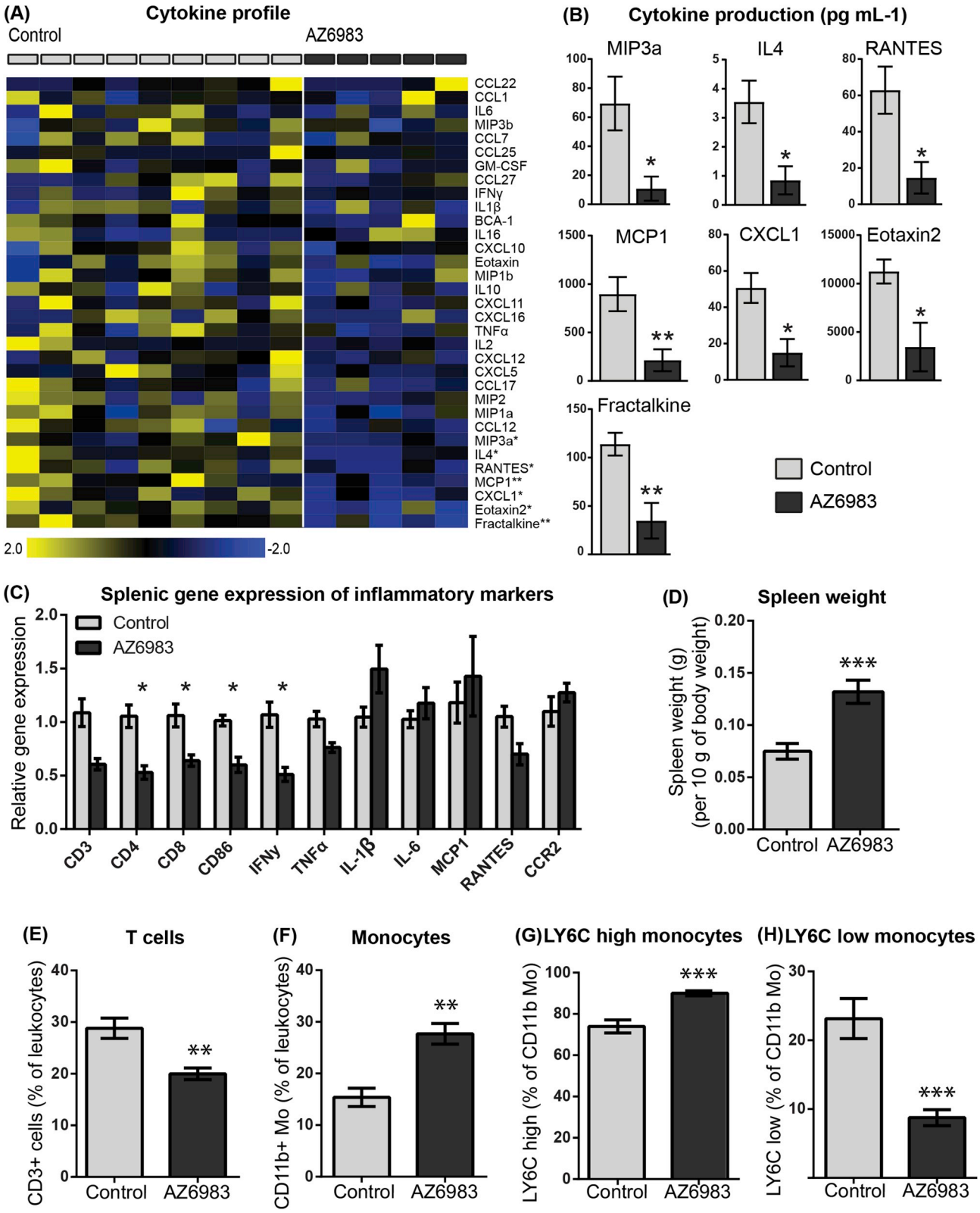

Fig. 4. AZ6983 regulates systemic inflammatory markers. *apoE*$^{-/-}$ mice treated with 50 μmol kg-1 per day of AZ6983 or vehicle in osmotic minipumps for 8 weeks. (A-B) Cytokine concentration in serum was analyzed by Luminex and presented as a (A) heatmap for all cytokines and (B) bar graphs representing cytokines that were significantly different between the treatment group (n = 5) and controls (n = 9) using the Mann-Whitney *U* test. Non-detectable concentrations for individual animals were estimated to the lowest detectable standard concentration divided by a factor 8. (C) Relative mRNA expression for genes associated with inflammatory cells and cytokines was evaluated with real-time PCR in spleen. (D) Spleen weight presented as spleen weight (g) per 10 g of body weight. (E-H) Cell populations in spleen investigated with flow cytometry. (E-F) CD3^{+} cells and CD11b^{+} monocytes (Mo) are presented as % of leukocytes. (G-H) Subpopulations of monocytes were characterized as LY6C^{high} or LY6C^{low} and presented as % of monocytes. All data expressed as mean ± SEM. *$p < 0.05$, **$p < 0.01$, ***$p < 0.001$, n = 5–12/group.

Table 1
Cholesterol levels, organ injury markers, body weight and AZ6983 drug exposure.

			12-week study			8-week study		
			Control	AZ6983	Sign.	Control	AZ6983	Sign.
Total cholesterol	(mmol L-1)	*4 weeks*	16.9 ± 1.1	15.7 ± 1.4	ns	-	-	-
		8 weeks	14.9 ± 1.2	18.4 ± 1.8	*	26.2 ± 3.2	12.0 ± 0.8	***
		12 weeks	19.1 ± 1.8	16.8 ± 1.6	ns	-	-	-
Free cholesterol	(mmol L-1)	*8 weeks*	-	-	-	7.9 ± 0.5	5.5 ± 0.6	*
LDL cholesterol	(mmol L-1)	*8 weeks*	-	-	-	12.5 ± 0.9	6.5 ± 1.1	***
Creatinine	(mg/L)	*8 weeks*	-	-	-	87.4 ± 11.6	87.9 ± 22.2	ns
ALT	(ng/ml)	*8 weeks*	-	-	-	1.87 ± 0.12	1.64 ± 1.33	ns
Body weight	(g)	*4 weeks*	26.6 ± 1.5	25.7 ± 0.5	ns	31.4 ± 0.8	31.5 ± 0.7	ns
		8 weeks	30.5 ± 1.9	29.2 ± 1.2	ns	33.6 ± 1.2	31.6 ± 1.1	ns
		12 weeks	33.7 ± 2.1	31.6 ± 1.7	ns	-	-	-
AZ6983	(μmol L-1)	*4 weeks*	-	0.36 ± 0.015	-	-	0.45 ± 052	-
		8 weeks	-	0.38 ± 0.026	-	-	0.67 ± 0.12	-

ApoE$^{-/-}$ mice were treated with AZ6983 admixed in diet or control diet for 12 weeks, or AZ6983 or vehicle through minipumps for 8 weeks. Total cholesterol, free cholesterol, LDL cholesterol, creatinine and alanine transaminase (ALT) were measured in plasma (12-week study) or serum (8 weeks study). AZ6983 exposure was measured in plasma (12-week study) or in whole blood (8-week study). All data is expressed as mean ± SEM. *$p < 0.05$, **$p < 0.01$, ***$p < 0.001$, ns = not significant, n = 8–12/group.

remains to be determined. In the study by Hashimoto et al. [12], AR-R17779 reduced total cholesterol and triglyceride levels, potentially contributing to the atheroprotective effects. In the current study, AZ6983 did not have a consistent effect on systemic cholesterol. AZ6983 increased total cholesterol after eight weeks, and gave no differences between the treatment groups at sacrifice in the 12-week study. In contrast, the treatment group had reduced total cholesterol at sacrifice in the 8-week study. This unexpected discrepancy needs to be investigated in future studies. The lipid profile was further investigated in the 8-week study, where a reduction in free cholesterol and LDL cholesterol was presented. Since LDL cholesterol is atherogenic, a lower fraction could contribute to less atherosclerosis in the 8-week study. However, in view of the contradictive cholesterol metrics in the 12-week study, cholesterol metabolism alone cannot explain the atheroprotective effects of AZ6983. To further identify the mechanisms behind the athero-protective effects of AZ6983, we performed gene expression analysis of aortas using RNA sequencing and pathway analysis. Interestingly, the top five specific functions suggested by the IPA analysis to be influenced by AZ6983 treatment included arteriosclerosis, adhesion of blood cells, binding of myeloid cells, phagocytosis of cells and engulfment of cells. A common feature for these functions is the involvement of myeloid cells. Indeed, monocytes play an important role in vascular inflammation, being the first cells recruited to the site of inflammation as well as contributing to local proliferation of tissue-specific macrophages [41,42]. Interestingly, α7nAChR-expressing macrophages has been attributed a central role in the cholinergic anti-inflammatory pathway [6,7], further proposing myeloid cells to be investigated for involvement in the link between α7nAChR activity and inhibition of atherosclerosis. Indeed, immunostaining of the atherosclerotic lesions revealed a decrease in CD68^{+} macrophages after AZ6983 treatment. Likewise, the proliferation marker Ki67 was significantly decreased, indicating a reduction in proliferating cells after treatment. Even though we cannot claim that this effect is myeloid cell specific, these findings are in line with previous studies that demonstrated that α7nAChR deficiency accelerated neointima formation, increased inflammation (macrophage marker CD68 and chemokines CCL2 and CXCL2) and increased proliferation in a vascular injury model [43]. Consistently, treatment of vascular injury with the α7nAChR agonist PNU-282987 inhibited neointima formation, decreased inflammation and reduced cell proliferation [43].

Another functional indication from the IPA analysis was phagocytosis and engulfment of cells, an important macrophage feature in the development of atherosclerosis and an essential part of the resolution of inflammation [44]. It was recently shown that restoring phagocytosis, by blocking the anti-phagocytic molecule CD47, decreases atherosclerosis [45]. CD47 is expressed by viable cells under normal conditions and is down-regulated during apoptosis, allowing the cells to be phagocytosed. However, CD47 expression is increased in advanced atherosclerosis [45]. In this study, CD47 was decreased in the lesions of mice treated with AZ6983, indicating that the clearance of apoptotic cells might be enhanced. The capability of macrophages to engage in phagocytosis might not only be dependent on phagocytic stimuli from apoptotic cells and debris, but also their inherent capacity to phagocytose. In a previous study, α7nAChR agonist GTS-21 restored phagocytosis of bacteria in LPS-stimulated RAW 264.7 macrophages [46]. The present study adds to the literature by demonstrating that α7nAChR-stimulation also improves the phagocytic properties of bone marrow-derived macrophages by increasing their capacity to engulf latex particles. Even more important, AZ6983 proved to increase the frequency of macrophages that could phagocyte apoptotic macrophages, a key function in efferocytosis [44]. These effects are modest, yet very robust.

The development of atherosclerosis is highly dependent on the recruitment of myeloid cells, their binding to the vessel wall, and trans-endothelial migration [47]. The present IPA analysis presented “adhesion of cells” and “binding of myeloid cells” as functions that could have been affected by the AZ6983 treatment. Vascular adhesion molecules are imperative for the transendothelial migration and the vascular adhesion molecule 1 (VCAM-1) is closely correlated with monocyte-derived cell infiltration and lesion formation [48,49]. We did not detect any treatment effects on expression of VCAM-1 in atherosclerotic lesions, however, it is plausible that other adhesion molecules might be affected. Another requirement for cells to adhere to the endothelium is their chemotactical guidance to the site of inflammation by cytokines [50]. Indeed, serum analysis of a broad range of cytokines revealed that AZ983 treatment caused a dramatic decrease in chemokines with established pro-atherogenic effects, including MIP3a (CCL20), IL-4, RANTES (CCL5), MCP1 (CCL2), CXCL1 (GROα), Eotaxin-2 (CCL24) and Fractalkine (CX3CL1) [13–17,51,52]. Interestingly, the majority of these cytokines (RANTES, MCP1, CXCL1, and Fractalkine) are chemokines involved in the vascular recruitment of myeloid cells [13,15–17]. We suggest that a systemic reduction of these chemokines could inhibit monocytes mobility to inflamed vessels and subsequent infiltration, potentially explaining the reduction of lesion macrophages. Immunohistochemistry of chemokines inside the lesions strengthens this theory by displaying a reduction of monocyte chemoattractant protein-1 (MCP1). Even though lesion CXCL1 was not significantly affected by the treatment, this indicates that AZ6983 has a local effect on chemokine release in the lesions, reducing the recruitment of myeloid cells into the atherosclerotic lesions. In the current study, myeloid markers

of chemotaxis were also investigated in the spleen where the gene expression for RANTES and MCP1 was determined, however, no treatment effects were identified. Besides circulating in the blood, monocytes also reside in the bone marrow and spleen [53] where splenic monocytes contribute to atherogenesis [41]. Since the spleen has been attributed an important role in α7nAChR-mediated anti-inflammatory responses [7] we aimed to assess the splenic status after treatment with AZ6983. Quite surprisingly, AZ6983 treatment increased spleen weight. One can only speculate about the underlying cause, however, since vascular atherosclerosis, systemic cytokines and pro-inflammatory gene expression in the spleen were decreased by the treatment, we propose that the splenomegaly is not due to increased immune activation. In line with this, analysis of the liver enzyme ALT and serum creatinine indicated that liver and kidney function were unaffected by the treatment. Interestingly, the frequency of splenic CD11b $^{+}$ monocytes were increased by AZ6983 treatment and shifted towards a Ly6C^{high} subtype. Ly6C^{high} monocytes are regarded as inflammatory and infiltrate injured tissues and predominate the recruitment to inflamed vessels. In contrary, Ly6C^{low} monocytes patrol healthy tissue and are regarded as cells which may participate in resolution of inflammation [54–56]. It has been shown that monocytes can be released from the splenic reservoir upon injury [57]. Given the anti-inflammatory effects of AZ6983 we speculate that pro-inflammatory monocytes could be retained within the splenic reservoir during α7nAChR stimulation, and not released into the circulation where they are recruited to the atherosclerotic lesions. However, the association between splenic monocyte retention and spleen weight needs further investigation. Of note, it should be considered that monocyte frequency may not reflect their total numbers in the spleen and a limitation of the current study is the lack of information regarding monocyte numbers in spleen, bone marrow and the circulation. The present IPA-analysis implied modulated innate immune responses in the aorta to be central in AZ6983 treatment. In line with this, immunostaining for CD3^{+} T cells in the aortic root was unaffected after AZ6983 treatment. However, T cell associated cytokines IL-4 and MIP3a (CCL20) were decreased in serum and several T cell associated markers were reduced after AZ6983 treatment in the spleen on both gene and protein level. We cannot determine if the non-vascular effects on T cells are direct effects of AZ6983 on the adaptive immune system or if it is a consequence of modulated myeloid response. The reduction of splenic CD86 mRNA could imply that treatment effects on monocytes, or other antigen-presenting cells, further inhibits adaptive immune responses since CD86 is a necessary co-stimulator for T-cell activation [58].

In conclusion, the novel α7nAChR agonist AZ6983 effectively decreases atherosclerosis and lesion macrophages in *apoE*$^{-/-}$ mice. AZ6983 treatment reduces inflammation locally in the atherosclerotic lesion and in inflamed compartments, as well as systemically, by suppressing chemokines with well-established roles in atherosclerosis and myeloid chemotaxis. Further, AZ6983 improves phagocytosis of apoptotic macrophages *in vitro* and reduces anti-phagocytic signals in lesions. Thus, we suggest that the anti-atherosclerotic effect of α7nAChR stimulation may be caused by modulation of myeloid immune cell responses where reduced cell recruitment into lesions and improved efferocytosis could be central mechanisms. The anti-inflammatory effect of AZ6983 in human blood further strengthens the α7nAChR as a potential target to treat human disease.

Conflicts of interest

The authors declared they do not have anything to disclose regarding conflict of interest with respect to this manuscript.

Financial support

Our work was supported by grants from The Swedish Heart Lung foundation, The Swedish Research Council, The Swedish Society of Medicine, Magnus Bergvall foundation, Stiftelsen Längmanska kulturfonden, Stiftelsen Gamla tjänarinnor, Lars Hiertas foundation, Åke Wiberg foundation, OE and Edla Johanssons vetenskapliga stiftelse, Stiftelsen Tornspiran, Emil and Wera Cornells foundation, Dr. Felix Neubergh Foundation, Emelle Foundation, Wilhelm and Martina Lundgren foundation and grants from the Swedish state under the agreement between the Swedish government and the county councils, the ALF-agreement (ALF GBG-723131).

Author contributions

M.A.U, F.M., E.M and M.E.J. designed the study, executed the experiments and wrote the manuscript. D.P., L.J.Y, K.E., S.G. and Y.W. performed experiments. M.A.U, F.M., L.M.G., H.N., E.M and M.E.J provided intellectual input and revised the manuscript. All authors reviewed the final manuscript.

Acknowledgements

We are grateful for the excellent technical and administrative assistance from Ms Sansan Hua, Mr Peter Micallef, Mrs Margareta Behrendt and Dr. Ann-Cathrine Jönsson-Rylander. The authors would like to acknowledge data analysis support from the Bioinformatics Core Facility at the Sahlgrenska Academy.

Appendix A. Supplementary data

Supplementary data to this article can be found online at https://doi.org/10.1016/j.atherosclerosis.2019.06.903.

References

[1] G.K. Hansson, A. Hermansson, The immune system in atherosclerosis, Nat. Immunol. 12 (3) (2011) 204–212, https://doi.org/10.1038/ni.2001.
[2] H.V. Huikuri, V. Jokinen, M. Syvanne, M.S. Nieminen, K.E. Airaksinen, M.J. Ikaheimo, ... M.H. Frick, Heart rate variability and progression of coronary atherosclerosis, Arterioscler. Thromb. Vasc. Biol. 19 (8) (1999) 1979–1985.
[3] R.E. Kleiger, J.P. Miller, J.T. Bigger Jr., A.J. Moss, Decreased heart rate variability and its association with increased mortality after acute myocardial infarction, Am. J. Cardiol. 59 (4) (1987) 256–262.
[4] H. Tsuji, M.G. Larson, F.J. Venditti Jr., E.S. Manders, J.C. Evans, C.L. Feldman, D. Levy, Impact of reduced heart rate variability on risk for cardiac events. The Framingham Heart Study, Circulation 94 (11) (1996) 2850–2855.
[5] M.A. Ulleryd, U. Prahl, J. Borsbo, C. Schmidt, S. Nilsson, G. Bergstrom, M.E. Johansson, The association between autonomic dysfunction, inflammation and atherosclerosis in men under investigation for carotid plaques, PLoS One 12 (4) (2017) e0174974, , https://doi.org/10.1371/journal.pone.0174974.
[6] L.V. Borovikova, S. Ivanova, M. Zhang, H. Yang, G.I. Botchkina, L.R. Watkins, ... K.J. Tracey, Vagus nerve stimulation attenuates the systemic inflammatory response to endotoxin, Nature 405 (6785) (2000) 458–462.
[7] H. Wang, M. Yu, M. Ochani, C.A. Amella, M. Tanovic, S. Susarla, ... K.J. Tracey, Nicotinic acetylcholine receptor [alpha]7 subunit is an essential regulator of inflammation, Nature 421 (6921) (2003) 384–388.
[8] M.E. Johansson, M.A. Ulleryd, A. Bernardi, A.M. Lundberg, A. Andersson, L. Folkersen, ... G.K. Hansson, alpha7 Nicotinic acetylcholine receptor is expressed in human atherosclerosis and inhibits disease in mice–brief report, Arterioscler. Thromb. Vasc. Biol. 34 (12) (2014) 2632–2636, https://doi.org/10.1161/atvbaha.114.303892.
[9] R.H. Lee, G. Vazquez, Reduced size and macrophage content of advanced atherosclerotic lesions in mice with bone marrow specific deficiency of alpha 7 nicotinic acetylcholine receptor, PLoS One 10 (3) (2015) e0124584, , https://doi.org/10.1371/journal.pone.0124584.
[10] S. Kooijman, I. Meurs, M. van der Stoep, K.L. Habets, B. Lammers, J.F.P. Berbée, ... P.C.N. Rensen, Hematopoietic α7 nicotinic acetylcholine receptor deficiency increases inflammation and platelet activation status, but does not aggravate atherosclerosis, J. Thromb. Haemost. 13 (1) (2015) 126–135, https://doi.org/10.1111/jth.12765.
[11] A. Al-Sharea, M.K.S. Lee, A. Whillas, M.C. Flynn, J. Chin-Dusting, A.J. Murphy, Nicotinic acetylcholine receptor alpha 7 stimulation dampens splenic myelopoiesis and inhibits atherogenesis in Apoe(-/-) mice, Atherosclerosis 265 (2017) 47–53, https://doi.org/10.1016/j.atherosclerosis.2017.08.010.
[12] T. Hashimoto, T. Ichiki, A. Watanabe, E. Hurt-Camejo, E. Michaelsson, J. Ikeda, ... K. Sunagawa, Stimulation of alpha7 nicotinic acetylcholine receptor by AR-R17779 suppresses atherosclerosis and aortic aneurysm formation in apolipoprotein E-deficient mice, Vasc. Pharmacol. 61 (2–3) (2014) 49–55, https://doi.org/10.1016/j.vph.2014.03.006.

[13] R.J. Aiello, P.A. Bourassa, S. Lindsey, W. Weng, E. Natoli, B.J. Rollins, P.M. Milos, Monocyte chemoattractant protein-1 accelerates atherosclerosis in apolipoprotein E-deficient mice, Arterioscler. Thromb. Vasc. Biol. 19 (6) (1999) 1518–1525.

[14] O. Calvayrac, R. Rodríguez-Calvo, J. Alonso, J. Orbe, J.L. Martín-Ventura, A. Guadall, ... J. Martínez-González, CCL20 is increased in hypercholesterolemic subjects and is upregulated by LDL in vascular smooth muscle cells, Arterioscler. Thromb. Vasc. Biol. 31 (11) (2011) 2733–2741, https://doi.org/10.1161/ATVBAHA.111.235721.

[15] A. Schober, D. Manka, P. von Hundelshausen, Y. Huo, P. Hanrath, I.J. Sarembock, C. Weber, Deposition of platelet RANTES triggering monocyte recruitment requires P-selectin and is involved in neointima formation after arterial injury, Circulation 106 (12) (2002) 1523–1529.

[16] O. Soehnlein, M. Drechsler, Y. Doring, D. Lievens, H. Hartwig, K. Kemmerich, C. Weber, Distinct functions of chemokine receptor axes in the atherogenic mobilization and recruitment of classical monocytes, EMBO Mol. Med. 5 (3) (2013) 471–481, https://doi.org/10.1002/emmm.201201717.

[17] F. Tacke, D. Alvarez, T.J. Kaplan, C. Jakubzick, R. Spanbroek, J. Llodra, G.J. Randolph, Monocyte subsets differentially employ CCR2, CCR5, and CX3CR1 to accumulate within atherosclerotic plaques, J. Clin. Investig. 117 (1) (2007) 185–194, https://doi.org/10.1172/jci28549.

[18] R.G. Gerrity, The role of the monocyte in atherogenesis: I. Transition of blood-borne monocytes into foam cells in fatty lesions, Am. J. Pathol. 103 (2) (1981) 181–190.

[19] D.M. Schrijvers, G.R. De Meyer, A.G. Herman, W. Martinet, Phagocytosis in atherosclerosis: molecular mechanisms and implications for plaque progression and stability, Cardiovasc. Res. 73 (3) (2007) 470–480, https://doi.org/10.1016/j.cardiores.2006.09.005.

[20] M.E. Johansson, A. Wickman, S.M. Fitzgerald, L.M. Gan, G. Bergstrom, Angiotensin II, type 2 receptor is not involved in the angiotensin II-mediated pro-atherogenic process in ApoE-/- mice, J. Hypertens. 23 (8) (2005) 1541–1549.

[21] C.S. Elmore, S. Landvatter, P.N. Dorff, M.E. Powell, D. Killick, T. Blake, ... G. Ernst, Synthesis of three alpha 7 agonists in labeled form, J. Label. Comp. Radiopharm. 57 (5) (2014) 342–349, https://doi.org/10.1002/jlcr.3186.

[22] Y. Kojima, I.L. Weissman, N.J. Leeper, The role of efferocytosis in atherosclerosis, Circulation 135 (5) (2017) 476–489, https://doi.org/10.1161/circulationaha.116.025684.

[23] M.A. Ulleryd, F. Mjornstedt, D. Panagaki, L.J. Yang, K. Engevall, S. Gutierrez, ... M.E. Johansson, RNA Sequencing Data Describing Transcriptional Changes in Aorta of ApoE-/- Mice after Alpha 7 Nicotinic Acetylcholine Receptor (α7nAChR) Stimulation, Data in Brief, Submitted, 2019.

[24] M. Rosas-Ballina, M. Ochani, W.R. Parrish, K. Ochani, Y.T. Harris, J.M. Huston, ... K.J. Tracey, Splenic nerve is required for cholinergic antiinflammatory pathway control of TNF in endotoxemia, Proc. Natl. Acad. Sci. Unit. States Am. 105 (31) (2008) 11008–11013, https://doi.org/10.1073/pnas.0803237105.

[25] A. Bruchfeld, R.S. Goldstein, S. Chavan, N.B. Patel, M. Rosas-Ballina, N. Kohn, ... K.J. Tracey, Whole blood cytokine attenuation by cholinergic agonists ex vivo and relationship to vagus nerve activity in rheumatoid arthritis, J. Intern. Med. 268 (1) (2010) 94–101, https://doi.org/10.1111/j.1365-2796.2010.02226.x.

[26] M. Rosas-Ballina, R.S. Goldstein, M. Gallowitsch-Puerta, L. Yang, S. Valdés-Ferrer, N.B. Patel, ... K.J. Tracey, The selective α7 agonist GTS-21 attenuates cytokine production in human whole blood and human monocytes activated by ligands for TLR2, TLR3, TLR4, TLR9, and RAGE, Mol. Med. 15 (7–8) (2009) 195–202, https://doi.org/10.2119/molmed.2009.00039.

[27] O. Borst, M. Schaub, B. Walker, E. Schmid, P. Munzer, J. Voelkl, ... F. Lang, Pivotal role of serum- and glucocorticoid-inducible kinase 1 in vascular inflammation and atherogenesis, Arterioscler. Thromb. Vasc. Biol. 35 (3) (2015) 547–557, https://doi.org/10.1161/atvbaha.114.304454.

[28] H.D. Manthey, C. Cochain, S. Barnsteiner, E. Karshovska, J. Pelisek, M. Koch, ... A. Zernecke, CCR6 selectively promotes monocyte mediated inflammation and atherogenesis in mice, Thromb. Haemostasis 110 (6) (2013) 1267–1277, https://doi.org/10.1160/th13-01-0017.

[29] A.J. Narasimha, J. Watanabe, T.O. Ishikawa, S.J. Priceman, L. Wu, H.R. Herschman, S.T. Reddy, Absence of myeloid COX-2 attenuates acute inflammation but does not influence development of atherosclerosis in apolipoprotein E null mice, Arterioscler. Thromb. Vasc. Biol. 30 (2) (2010) 260–268, https://doi.org/10.1161/atvbaha.109.198762.

[30] A. Rossignoli, M.M. Shang, H. Gladh, C. Moessinger, H. Foroughi Asl, H.A. Talukdar, ... J. Skogsberg, Poliovirus receptor-related 2: a cholesterol-responsive gene affecting atherosclerosis development by modulating leukocyte migration, Arterioscler. Thromb. Vasc. Biol. 37 (3) (2017) 534–542, https://doi.org/10.1161/atvbaha.116.308715.

[31] G. Camussi, E. Albano, C. Tetta, F. Bussolino, The molecular action of tumor necrosis factor-alpha, Eur. J. Biochem. 202 (1) (1991) 3–14.

[32] D.A. Griffiths-Johnson, P.D. Collins, A.G. Rossi, P.J. Jose, T.J. Williams, The chemokine, eotaxin, activates Guinea-pig eosinophils *in vitro* and causes their accumulation into the lung in vivo, Biochem. Biophys. Res. Commun. 197 (3) (1993) 1167–1172.

[33] E.A. Heller, E. Liu, A.M. Tager, Q. Yuan, A.Y. Lin, N. Ahluwalia, ... R.E. Gerszten, Chemokine CXCL10 promotes atherogenesis by modulating the local balance of effector and regulatory T cells, Circulation 113 (19) (2006) 2301–2312, https://doi.org/10.1161/CIRCULATIONAHA.105.605121.

[34] M.D. Miller, M.S. Krangel, The human cytokine I-309 is a monocyte chemoattractant, Proc. Natl. Acad. Sci. U. S. A 89 (7) (1992) 2950–2954.

[35] B.E. Hunter, C.M. de Fiebre, R.L. Papke, W.R. Kem, E.M. Meyer, A novel nicotinic agonist facilitates induction of long-term potentiation in the rat hippocampus, Neurosci. Lett. 168 (1–2) (1994) 130–134.

[36] E.M. Meyer, A. Kuryatov, V. Gerzanich, J. Lindstrom, R.L. Papke, Analysis of 3-(4-hydroxy, 2-Methoxybenzylidene)anabaseine selectivity and activity at human and rat alpha-7 nicotinic receptors, J. Pharmacol. Exp. Ther. 287 (3) (1998) 918–925.

[37] B.K. Garg, R.H. Loring, GTS-21 has cell-specific anti-inflammatory effects independent of alpha7 nicotinic acetylcholine receptors, PLoS One 14 (4) (2019) e0214942, , https://doi.org/10.1371/journal.pone.0214942.

[38] G. Mullen, J. Napier, M. Balestra, T. DeCory, G. Hale, J. Macor, ... J. Gordon, (−)-Spiro[1-azabicyclo[2.2.2]octane-3,5‘-oxazolidin-2‘-one], a conformationally restricted analogue of acetylcholine, is a highly selective full agonist at the α7 nicotinic acetylcholine receptor, J. Med. Chem. 43 (22) (2000) 4045–4050, https://doi.org/10.1021/jm000249r.

[39] D. Bertrand, C.-H.L. Lee, D. Flood, F. Marger, D. Donnelly-Roberts, Therapeutic potential of < em > α < /em > 7 nicotinic acetylcholine receptors, Pharmacol. Rev. 67 (4) (2015) 1025–1073, https://doi.org/10.1124/pr.113.008581.

[40] R.L. Papke, J.K. Porter Papke, G.M. Rose, Activity of alpha7-selective agonists at nicotinic and serotonin 5HT3 receptors expressed in Xenopus oocytes, Bioorg. Med. Chem. Lett 14 (8) (2004) 1849–1853, https://doi.org/10.1016/j.bmcl.2003.09.104.

[41] C.S. Robbins, A. Chudnovskiy, P.J. Rauch, J.L. Figueiredo, Y. Iwamoto, R. Gorbatov, ... F.K. Swirski, Extramedullary hematopoiesis generates Ly-6C(high) monocytes that infiltrate atherosclerotic lesions, Circulation 125 (2) (2012) 364–374, https://doi.org/10.1161/circulationaha.111.061986.

[42] V.I. Sayin, O.M. Khan, L.E. Pehlivanoglu, A. Staffas, M.X. Ibrahim, A. Asplund, ... P. Lindahl, Loss of one copy of Zfp148 reduces lesional macrophage proliferation and atherosclerosis in mice by activating p53, Circ. Res. 115 (9) (2014) 781–789, https://doi.org/10.1161/circresaha.115.304992.

[43] D.J. Li, H. Fu, J. Tong, Y.H. Li, L.F. Qu, P. Wang, F.M. Shen, Cholinergic anti-inflammatory pathway inhibits neointimal hyperplasia by suppressing inflammation and oxidative stress, Redox Biol 15 (2018) 22–33, https://doi.org/10.1016/j.redox.2017.11.013.

[44] I. Tabas, Macrophage death and defective inflammation resolution in atherosclerosis, Nat. Rev. Immunol. 10 (1) (2010) 36–46, https://doi.org/10.1038/nri2675.

[45] Y. Kojima, J.P. Volkmer, K. McKenna, M. Civelek, A.J. Lusis, C.L. Miller, ... N.J. Leeper, CD47-blocking antibodies restore phagocytosis and prevent atherosclerosis, Nature 536 (7614) (2016) 86–90, https://doi.org/10.1038/nature18935.

[46] R.A. Sitapara, D.J. Antoine, L. Sharma, V.S. Patel, C.R. Ashby Jr., S. Gorasiya, ... L.L. Mantell, The alpha7 nicotinic acetylcholine receptor agonist GTS-21 improves bacterial clearance in mice by restoring hyperoxia-compromised macrophage function, Mol. Med. 20 (2014) 238–247, https://doi.org/10.2119/molmed.2013.00086.

[47] G.K. Hansson, P. Libby, The immune response in atherosclerosis: a double-edged sword, Nat. Rev. Immunol. 6 (7) (2006) 508–519.

[48] Y. Nakashima, E.W. Raines, A.S. Plump, J.L. Breslow, R. Ross, Upregulation of VCAM-1 and ICAM-1 at atherosclerosis-prone sites on the endothelium in the ApoE-deficient mouse, Arterioscler. Thromb. Vasc. Biol. 18 (5) (1998) 842–851.

[49] A. Sakai, N. Kume, E. Nishi, K. Tanoue, M. Miyasaka, T. Kita, P-selectin and vascular cell adhesion molecule-1 are focally expressed in aortas of hypercholesterolemic rabbits before intimal accumulation of macrophages and T lymphocytes, Arterioscler. Thromb. Vasc. Biol. 17 (2) (1997) 310–316.

[50] A. Zernecke, C. Weber, Chemokines in atherosclerosis, Arterioscler. Thromb. Vasc. Biol. 34 (4) (2014) 742–750, https://doi.org/10.1161/ATVBAHA.113.301655.

[51] P. Davenport, P.G. Tipping, The role of interleukin-4 and interleukin-12 in the progression of atherosclerosis in apolipoprotein E-deficient mice, Am. J. Pathol. 163 (3) (2003) 1117–1125 https://doi.org/10.1016/S0002-9440(10)63471-2.

[52] C.-S. Tsai, C.-Y. Huang, C.-H. Chen, Y.-W. Lin, C.-M. Shih, N.-W. Tsao, ... F.-Y. Lin, Eotaxin-2 increased toll-like receptor 4 expression in endothelial cells *in vitro* and exacerbates high-cholesterol diet-induced atherogenesis in vivo, Am. J. Transl. Res. 8 (12) (2016) 5338–5353.

[53] K.J. Woollard, F. Geissmann, Monocytes in atherosclerosis: subsets and functions, Nat. Rev. Cardiol. 7 (2) (2010) 77–86, https://doi.org/10.1038/nrcardio.2009.228.

[54] C. Auffray, D. Fogg, M. Garfa, G. Elain, O. Join-Lambert, S. Kayal, F. Geissmann, Monitoring of blood vessels and tissues by a population of monocytes with patrolling behavior, Science 317 (5838) (2007) 666–670, https://doi.org/10.1126/science.1142883.

[55] M. Nahrendorf, F.K. Swirski, E. Aikawa, L. Stangenberg, T. Wurdinger, J.L. Figueiredo, ... M.J. Pittet, The healing myocardium sequentially mobilizes two monocyte subsets with divergent and complementary functions, J. Exp. Med. 204 (12) (2007) 3037–3047, https://doi.org/10.1084/jem.20070885.

[56] F.K. Swirski, P. Libby, E. Aikawa, P. Alcaide, F.W. Luscinskas, R. Weissleder, M.J. Pittet, Ly-6Chi monocytes dominate hypercholesterolemia-associated monocytosis and give rise to macrophages in atheromata, J. Clin. Investig. 117 (1) (2007) 195–205, https://doi.org/10.1172/jci29950.

[57] F.K. Swirski, M. Nahrendorf, M. Etzrodt, M. Wildgruber, V. Cortez-Retamozo, P. Panizzi, ... M.J. Pittet, Identification of splenic reservoir monocytes and their deployment to inflammatory sites, Science 325 (5940) (2009) 612–616, https://doi.org/10.1126/science.1175202.

[58] S. Mukherjee, P.K. Maiti, D. Nandi, Role of CD80, CD86, and CTLA4 on mouse CD4(+) T lymphocytes in enhancing cell-cycle progression and survival after activation with PMA and ionomycin, J. Leukoc. Biol. 72 (5) (2002) 921–931.